not ovalbumin as a control. The factor appears to be unrelated to the currently identified R5 HIV-1 suppressive cytokines examined by neutralization assay using antibodies against CCR5-binding β-chemokines, IL-4, IL-10, IL-12, IL-13, IL-16, MCP-1, MCP-3, IFN-α, IFN-β, TNF-α, and TNF-β.

Our study indicates that a DC-based HIV-1 vaccination can induce HIV-1-reactive human $CD4^+$ T cells producing a yet-undefined R5 HIV-1 suppressor factor. The demonstration made by Lu et al. (Lu et al. 2003) that DC pulsed with AT-2 inactivated simian immunodeficiency virus (SIV) can also stimulate protective anti-SIV specific T cell and antibody responses in rhesus monkeys suggests a rational basis for the DC-based immunization against HIV-1 infection. This idea is further supported by the recent findings by Lu et al. (Lu et al. 2004), who showed the efficacy of a therapeutic DC-based whole HIV-1 virion vaccination for HIV-1 infection.

In order to achieve successful DC-based immunization against HIV-1, a large number of monocyte-derived mature DC with immuno-stimulating activity is expected. A conventional method for generating DC from monocytes has been established, and there are commercially available kits for monocyte purification. In addition, we recently found a simple method to isolate monocytes from bulk PBMC by using antichemokine receptor monoclonal antibody-coated plates (Nimura et al. 2006). These monocytes could be differentiated to Th1-inducing DC and expressed low levels of cell surface CD4 and CCR5. When sensitized with inactivated HIV-1, these DC could induce the R5 HIV-1-suppressing factor in the hu-PBL-SCID mouse (Nimura et al. 2006). Because human monocytes and immature DC are still susceptible to R5 HIV-1 infection, this method, which can induce HIV-1-resistant DC, will be helpful for HIV-1-infected individuals in generation of therapeutic DC against acquired immunodeficiency syndrome (AIDS).

2 Development of Immunodeficient Mouse Strains for Improvement of Human Cell Reconstitution and HIV-1 Infection

2.1 Generation of Novel Immunodeficient Mouse Strains

By introduction of the *scid/scid* mutation in various strains of inbred mice possessing defects in innate immunity, we surveyed congenic mouse strains to find an adequate immunodeficient mouse for transplantation of human cells and HIV-1 infection. From extensive transplantation experiments with human PBMC in immunodeficient mouse strains, the NOD-SCID mouse, which contains some defects in the function of complements and macrophages, was found to be a most suitable strain as a recipient for human cell reconstitution as well as HIV-1 infection (Koyanagi et al. 1997a). The number of human cells in the human PBMC-transplanted NOD-SCID (hu-PBL-NOD-SCID) mice was more than

three- to fivefold higher than that in the conventional hu-PBL-SCID mice. More importantly, the levels of HIV-1 viremia were significantly high in the HIV-1 infected hu-PBL-NOD-SCID mice. Some HIV-1-infected mice exhibited more than 1 ng of p24 antigen per milliliter in plasma, which is a much higher concentration than that in HIV-1-infected patients, and showed severe CD4 depletion after intraperitoneal inoculation with R5 HIV-1. Using this mouse model, we found that tumor necrosis factor (TNF)-related apoptosis-inducing ligand (TRAIL) but not Fas ligand induced bystander killing of $CD4^+$ T cells in the mouse spleen (Miura et al. 2001). In addition, when these HIV-1-infected mice were treated with a sublethal dose of lipopolysaccharide, HIV-1-infected cells migrated into mouse brain tissue and induced apoptosis in neuronal cells via TRAIL molecules expressed on the HIV-1-infected cells, probably macrophages (Miura et al. 2003). These data suggested that TRAIL should have a pathological role of disease progression for AIDS.

Recently, further genetic manipulation has been performed. A more profoundly severe immunodeficient mouse strain, defective in common γ (γ_c) chain, which is a component of receptors for IL-2, IL-7, and other cytokines and critical for generation of NK and T cells, was generated from the NOD-SCID mouse (Ito et al. 2002) and the recombination activating gene-2 (RAG-2)^{null} mouse. The RAG-2^{null} mouse is also a genetically manipulated immunodeficient strain, which has a defect in the differentiation of T and B cells. NOD-SCID γ_c^{null} (NOG) and RAG-2/γ_c^{null} mouse strains were then generated, and these mice have been confirmed to have neither functional T and B cell nor NK cells and have been used as humanized mouse models by transplantation of human immune cells. The level of human cell reconstitution was greatly improved in NOG as well as RAG-2/γ_c^{null} mice transplanted with human PBMC (hu-PBL-NOG and hu-PBL-RAG-2/γ_c^{null} mice) (Nakata et al. 2005; Koyanagi et al. 1997b). Moreover, a technical improvement should be noted in that it is not necessary for preceding treatment with antibody, an anti-IL-2 receptor β chain antibody or an anti-asialo GM-1 antibody, to protect mouse NK cell differentiation in recipient mice.

2.2 *HIV-1 Infection in the hu-PBL-NOG Mouse*

Using NOG mice, we indicated the usefulness of the mouse strain for evaluation of an anti-HIV-1 compound (Nakata et al. 2006). HIV-1 suppressive efficacy of a small molecule of CCR5 antagonist was confirmed in the mice 1 day after HIV-1 inoculation. The level of viral loads and HIV-1-induced CD4 depletion was dramatically suppressed after treatment of a CCR5 antagonist, suggesting that the NOG mouse should serve as a small animal model for evaluation of anti-HIV-1 compounds (Nakata at al. 2006). Furthermore, it is noteworthy that this hu-PBL-NOG model provides a greater reproducibility of high viremia levels than the conventional HIV-1-infected SCID mouse models and that the high level of viremia achieved in this mouse model made it possible to monitor the changes in the

viremia levels periodically in the same set of mice without sacrificing them, while most of the previously described SCID mouse models required mice to be sacrificed at each time point of testing (Mosier et al. 1993; Ruxrungtham et al. 1996; Strizki et al. 2001).

2.3 *Development of HSC-Engrafted Mouse for HIV-1 Infection*

Since human immune cells are not fully reconstituted in the chimeric mice transplanted with human PBMC, many researchers have been developing a improved immunodeficient mouse model engrafted with human HSC, which generates human T and B cells and also DC/macrophage myeloid cells for long periods of time and will be amenable to HIV-1 infection (Fig. 3). The HSC-engrafted mouse model allows mechanistic studies of HIV-1-induced disease progression, and possibly would allow analysis of immune responses derived from the human cells.

Using 8- to 10-week-old NOG mice engrafted with HSC or progenitor cells from cord blood, Nakahata and colleagues reported the significantly efficient reconstitution of human B cells as well as T cells in mice for more than 6 months (Hiramatsu et al. 2003). This successful engraftment (designated as the hNOG mouse) encouraged the subsequent HIV-1 infection experiment. We recently showed that in the hNOG mouse exhibiting long-lasting high levels of viremia and CD4 depletion in the peripheral blood were reproduced after both R5 and X4 HIV-1

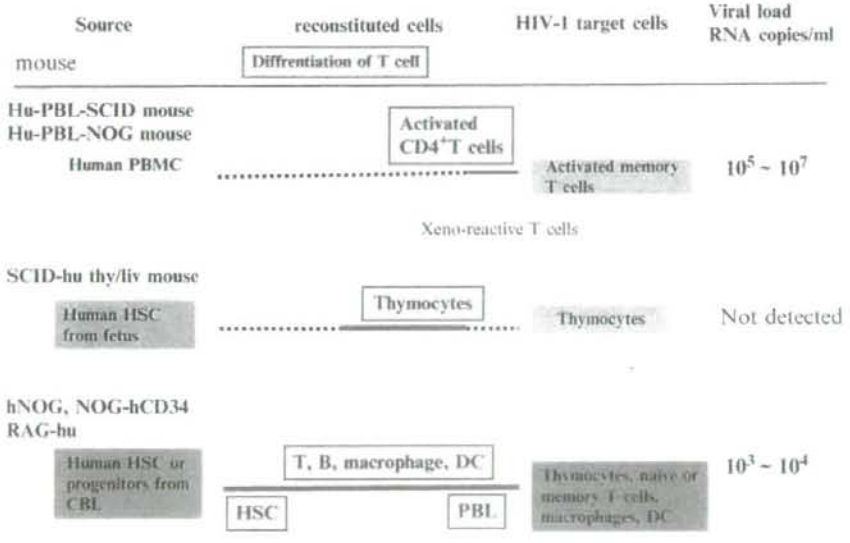

Fig. 3 Comparison of mouse/human chimeric models for HIV-1 infection. There have been three systems of humanized mouse models for HIV-1 infection

inoculation. Large amounts of HIV-1 DNA were detected in the spleen and bone marrow of R5 HIV-1-infected mice, and in the thymus and spleen of X4 virus-infected mice. Furthermore, anti-HIV p24 and gp120 antibodies were found in animals showing a high level of HIV-1 replication, indicating that HIV-1-specific immune response is induced in hNOG mice (Watanabe et al. 2007).

One modification of the CD34 engraftment into mice has been developed. Manz and colleagues reported that the newborn immunodeficient RAG-2/γ_c^{null} mouse strain is an adequate recipient for reconstitution of human immune cells including DC and that human adaptive immunity is clearly reconstituted in these mice (Traggiai et al. 2004). Another group also reported a significant improvement of human immune cell reconstitution with the newborn NOD/SCID/IL2 receptor γ chain^{null} mouse (Ishikawa et al. 2005). More recently, it was reported that efficient HIV-1 replication and CD4 depletion were shown in HSC-engrafted RAG-2/γ_c^{null} mice after HIV-1 inoculation (Baenziger et al. 2006; Berges et al. 2006; Zhang et al. 2007). We also confirmed that the engraftment procedure in newborn NOG mice with human CD34 created an HIV-1-susceptible mouse, and these mice (NOG-hCD34 mouse) after R5 or X4 HIV-1 inoculation possessed a level of viremia similar to that in HIV-1-infected patients. The NOG-hCD34 mice were also susceptible to infection with Epstein-Barr virus (EBV), which is known to be a human-specific γ herpes virus and to infect B cells. Several weeks after EBV inoculation, we could detect EBV DNA in the peripheral blood and spleen cells and could isolate EBV$^+$ lymphoblastoid cells from these mice (Koyanagi, unpublished observations).

3 Application of NOG Mice for HTLV Infection

3.1 HTLV

Human T-lymphotropic virus type I (HTLV-I) is another human retrovirus that causes adult T-cell leukemia (ATL)/ATL lymphoma and can also be involved in certain demyelinating diseases, tropical spastic paraparesis (TSP)/HTLV-I-associated myelopathy (HAM) (Hinuma et al. 1981; Osame et al. 1986). The malignant cells, mostly CD4$^+$ T cells, associated with all phases of ATL express very high levels of IL-2Rα (CD25) (Uchiyama et al. 1985). The median survival duration of all patients with aggressive ATL is about 13 months, and overall survival at 2 years is estimated to be about 30% (Taylor and Matsuoka 2005).

3.2 Model of HTLV-I-Induced Tumorigenicity

SCID mice have been utilized in a study on the pathomechanism and therapeutic strategy of ATL. Imada et al. examined the tumorigenicity of HTLV-I-infected cell

lines in an in vivo cell proliferation model using SCID mice. They found that 4 of 11 HTLV-I-infected cell lines were capable of proliferating in SCID mice after intraperitoneal inoculation. Interestingly, it was shown that some HTLV-I-infected and IL-2-dependent cell lines could be successfully engrafted in SCID mice (Imada et al. 1995). The expression of IL-2 mRNA was not detected in these cell lines growing either in vivo or in vitro. No HTLV-I viral structural proteins were detected in three of four transplantable cell lines proliferating in vivo. Peripheral blood T cells immortalized by introduction of *tax* gene of HTLV-I were found to have no tumorigenic potential in SCID mice. Although these systems were useful, two major drawbacks, namely, the long period of time required for tumor formation and the limitation of its use to certain cell lines, appear to hinder wider use of this animal model. These problems have now been overcome through development of the NOG mouse.

PBMC from patients with ATL were inoculated either intraperitoneally into the abdominal region or subcutaneously in the postauricular region of unconditional NOG mice. All mice developed clinical signs of near death, such as piloerection, weight loss, and cachexia, 6-8 weeks after inoculation of ATL cells in addition to enlargement of lymph nodes, spleen, lungs, and liver, whereas no tumors were found in the postauricular region or abdominal cavity where primary ATL cells were inoculated (Dewan et al. 2006). There was no difference in respect to the successful engraftment of ATL cells either intraperitoneally or subcutaneously inoculated into NOG mice. Histologic analysis of ATL-bearing mice showed massive infiltration of leukemic cells in various organs of NOG mice that were efficiently expressing human CD4 and CD25 molecules. A higher level of IL-2R (CD25) expression was observed on the surface of malignant cells associated with all stages of ATL as well as ATL cells infiltrated into various organs of patients. Thus, results from this model indicated successful engraftment and massive infiltration of primary ATL cells in various organs of NOG mice, like leukemia but without producing tumors at the sites of inoculation.

3.3 *Evaluation of Anti-*ATL *Compounds*

The various chemotherapies so far developed have not significantly increased the survival of patients with ATL (Taylor and Matsuoka 2005). Given the disappointing results using conventional chemotherapy, new approaches for the treatment of ATL are required. HTLV-I-infected cell lines derived from a leukemic cell clone and primary ATL cells failed to express significant amounts of Tax and other viral proteins, suggesting that the expression of viral proteins is not always necessary for leukemic proliferation at the late stage of the disease. However, HTLV-I-infected cell lines and leukemic cells from patients with ATL display constitutive NF-κB binding activity and increased degradation of a specific inhibitor, IκBα (Mori et al. 1999). NF-κB activation has been connected with multiple processes of oncogenesis, including control of apoptosis, cell cycle, differentiation, and cell migration; therefore, inhibition of NF-κB was suggested to be a useful strategy for cancer

therapy. Despite the diversity in clinical manifestations of ATL, strong and constitutive NF-κB activation was reported to be a unique and common characteristic of ATL cells (Mori et al. 1999). Thus, the indispensability of NF-κB for the maintenance of the malignant phenotype of HTLV-I provides a possible molecular target for ATL therapy. To study the effect of an NF-κB inhibitor, ritonavir, on ATL, we injected primary ATL cells from 10 patients subcutaneously into the postauricular region of NOG mice. Beginning 1 day after inoculation, mice were treated with either RPMI-1640 (as control) or ritonavir intraperitoneally daily for 30 days, followed by observation for another 30 days without any treatment. ATL cell inoculation promoted the development of piloerection, weight loss, and cachexia in addition to enlargement of lymph nodes, spleen, lungs, and liver in all control mice 2 months after inoculation. In contrast, ritonavir-treated mice were apparently healthy and had almost no enlargement of these organs. Clinical evaluation of organ invasion 2 months after injection of primary ATL cells showed that ritonavir treatment inhibited their infiltration into lymph nodes, spleen, lungs, and liver (Dewan et al. 2006). Seven of 10 patient samples injected in mice treated with ritonavir presented substantial inhibition of organ invasion, and 2 showed partial inhibition, whereas 1 sample failed to do so. In contrast, all control mice showed formation of new lymph nodes and infiltration with ATL cells into various organs. Organ infiltration of primary ATL cells was analyzed and evaluated by pathological staining and immunostaining of CD4 and CD25. We also performed similar experiments with HTLV-I-infected cell line cells [ED-40515(−), SLB-1, MT-1, TL-Oml, Hut-102, MT-2, and MT-4], using Bay 11-7082, which is another selective inhibitor of TNF-induced phosphorylation of IκBα without affecting the constitutive activation of IκBα phosphorylation, eventually resulting in decreased NF-κB and decreased expression of adhesion molecules (Dewan et al. 2003). Essentially, the same results were obtained in the studies using BAY11-7082 and the ED-40515(−) cell line. Together, these data indicate that NF-κB antagonists significantly inhibit ATL cell growth and infiltration in various organs of NOG mice.

Our NOG ATL model presents many features 6-8 weeks after inoculation of ATL cells such as the clinical signs observed in patients with ATL. Two clinical types, acute and chronic, carry very different prognoses. However, no difference in cell growth, surface phenotype, and NF-κB activity is observed in primary leukemic cells from patients with acute- and chronic-type ATL. Therefore, the same characteristics of freshly isolated ATL cells with acute- and chronic-type were observed in the NOG mouse. Thus, it represents a novel model to evaluate tissue toxicity and the efficacy of therapeutic agents directed toward the treatment of ATL (Fig. 4).

4 Concluding Remarks on Human Retrovirus Infection Model

The humanized mouse model should provide a midway position between the laboratory and clinical studies. From a relevant animal model for HIV and HTLV infections, immunological as well as virological aspects of the disease could be

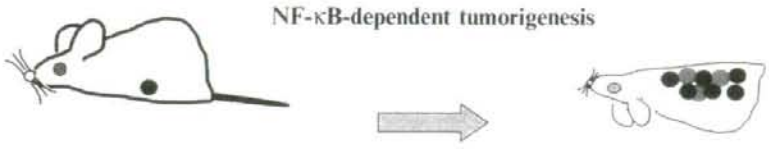

Clinical signs in NOG ATL model
Development to $CD4^+CD25^+$ lymphoma
Invasion of leukemic cells to multiple organs
Cachexia
No expression of HTLV-I proteins

Fig. 4 NOG ATL model. Model of HTLV-I-induced tumorigenicity is created with NOG mice. $HTLV^+$ T cells as well as primary ATL leukemic cells induce the identical clinical signs observed in patients with ATL.

investigated, and such an animal model could be used to examine the disease process and efficacy of antiviral compounds or vaccines. Significant progress in creating refined mouse strains has been achieved. We have now humanized mice, animals that circulate human blood. However, a mouse is not human. Therefore, there are still many limitations for examination of the human defense system. It is expected that the developments of technology in experimental animals and embryology, including methods using human ES or some other progenitor cells, will open the new evolution of humanized animals.

Acknowledgements This work was supported by grants from the Ministry of Health, Labor and Welfare, and the Ministry of Education, Culture, Sports, Science and Technology of Japan.

References

Aldrovandi GM, Feuer G, Gao L, Jamieson B, Kristeva M, Chen IS, Zack JA (1993) The SCID-hu mouse as a model for HIV-1 infection. Nature 363:732-736

Baenziger S, Tussiwand R, Schlaepfer E, Mazzucchelli L, Heikenwalder M, Kurrer MO, Behnke S, Frey J, Oxenius A, Joller H, Aguzzi A, Manz MG, Speck RF (2006) Disseminated and sustained HIV infection in CD34+ cord blood cell-transplanted Rag2−/−gamma c−/− mice. Proc Natl Acad Sci USA 103:15951-15956

Berges BK, Wheat WH, Palmer BE, Connick E, Akkina R (2006) HIV-1 infection and CD4 T cell depletion in the humanized Rag2−/−gamma c−/− (RAG-hu) mouse model. Retrovirology 3:76

Blunt T, Finnie NJ, Taccioli GE, Smith GC, Demengeot J, Gottlieb TM, Mizuta R, Varghese AJ, Alt FW, Jeggo PA et al. (1995) Defective DNA-dependent protein kinase activity is linked to VDJ recombination and DNA repair defects associated with the murine scid mutation. Cell 80:813-823

Bonyhadi ML, Rabin L, Salimi S, Brown DA, Kosek J, McCune JM, Kaneshima (1993) HIV induces thymus depletion in vivo. Nature 363:728-732

Bosma GC, Custer RP, Bosma MJ (1983) A severe combined immunodeficiency mutation in the mouse. Nature 301:527-530

Boubnov NV, Weaver DT (1995) scid cells are deficient in Ku and replication protein A phosphorylation by the DNA-dependent protein kinase. Mol Cell Biol 15:5700-5706

Delhem N, F Hadida, G Gorochov, F Carpentier, JP de Cavel, JF Andreani, B Autran, JY Cesbron (1998) Primary Th1 cell immunization against HIVgp160 in SCID-hu mice coengrafted with peripheral blood lymphocytes and skin. J Immunol 161:2060-2069

Dewan MZ, Terashima K, Taruishi M, Hasegawa H, Ito M, Tanaka Y, Mori N, Sata T, Koyanagi Y, Maeda M, Kubuki Y, Okayama A, Fujii M, Yamamoto N (2003) Rapid tumor formation of human T-cell leukemia virus type 1-infected cell lines in novel NOD-SCID/γc^{null} mice: suppression by an inhibitor against NF-kappaB. J Virol 77:5286-5294

Dewan MZ, Uchihara JN, Terashima K, Honda M, Sata T, Ito M, Fujii N, Uozumi K, Tsukasaki K, Tomonaga M, Kubuki Y, Okayama A, Toi M, Mori N, Yamamoto N (2006) Efficient intervention of growth and infiltration of primary adult T-cell leukemia cells by an HIV protease inhibitor, ritonavir. Blood 107:716-724

Gorantla S, Santos K, Meyer V, Dewhurst S, Bowers WJ, Federoff HJ, Gendelman HE, Poluektova L (2005) Human dendritic cells transduced with herpes simplex virus amplicons encoding human immunodeficiency virus type 1 (HIV-1) gp120 elicit adaptive immune responses from human cells engrafted into NOD/SCID mice and confer partial protection against HIV-1 challenge. J Virol 79:2124-2132

Hartley O, Gaertner H, Wilken J, Thompson D, Fish R, Ramos A, Pastore C, Dufour B, Cerini F, Melotti A, Heveker N, Picard L, Alizon M, Mosier D, Kent S, Offord R (2004) Medicinal chemistry applied to a synthetic protein: development of highly potent HIV entry inhibitors. Proc Natl Acad Sci USA 101:16460-16465

Hinuma Y, Nagata K, Hanaoka M, Nakai M, Matsumoto T, Kinoshita KI, Shirakawa S, Miyoshi I (1981) Adult T-cell leukemia: antigen in an ATL cell line and detection of antibodies to the antigen in human sera. Proc Natl Acad Sci USA 78:6476-6480

Hiramatsu H, Nishikomori R, Heike T, Ito M, Kobayashi K, Katamura K, Nakahata T (2003) Complete reconstitution of human lymphocytes from cord blood CD34+ cells using the NOD/SCID/γ_c^{null} mice model. Blood 102:873-880

Ifversen P, Borrebaeck CA (1996) SCID-hu-PBL: a model for making human antibodies? Semin Immunol 8:243-248

Imada K, Takaori-Kondo A, Akagi T, Shimotohno K, Sugamura K, Hattori T, Yamabe H, Okuma M, Uchiyama T (1995) Tumorigenicity of human T-cell leukemia virus type I-infected cell lines in severe combined immunodeficient mice and characterization of the cells proliferating in vivo. Blood 86:2350-2357

Ishikawa F, Yasukawa M, Lyons B, Yoshida S, Miyamoto T, Yoshimoto G, Watanabe T, Akashi K, Shultz LD, Harada M (2005) Development of functional human blood and immune systems in NOD/SCID/γ chain^{null} mice. Blood 106:1565-1573

Ito M, Hiramatsu H, Kobayashi K, Suzue K, Kawahata M, Hioki K, Ueyama Y, Koyanagi Y, Sugamura K, Tsuji K, Heike T, Nakahata T (2002) NOD/SCID/γ_c^{null} mouse: an excellent recipient mouse model for engraftment of human cells. Blood 100:3175-3182

Jamieson BD, Zack JA (1999) Murine models for HIV disease. AIDS 13 Suppl A:S5-11

Kaneshima H, Shih CC, Namikawa R, Rabin L, Outzen H, Machado SG, McCune JM (1991) Human immunodeficiency virus infection of human lymph nodes in the SCID/hu mouse. Proc Natl Acad Sci USA 88:4523-4527

Kaneshima H, Su L, Bonyhadi ML, Connor RI, Ho DD, McCune JM (1994) Rapid-high, syncytium-inducing isolates of human immunodeficiency virus type 1 induce cytopathicity in the human thymus of the SCID-hu mouse. J Virol 68:8188-8192

Kawano Y, Tanaka Y, Misawa N, Tanaka R, Kira JI, Kimura T, Fukushi M, Sano K, Goto T, Nakai M, Kobayashi T, Yamamoto N, Koyanagi Y (1997) Mutational analysis of human immunodeficiency virus type 1 (HIV-1) accessory genes: requirement of a site in the nef gene for HIV-1 replication in activated CD4+ T cells in vitro and in vivo. J Virol 1:8456-8466

Kirchgessner CU, Patil CK, Evans JW, Cuomo CA, Fried LM, Carter T, Oettinger MA, Brown JM (1995) DNA-dependent kinase (p350) as a candidate gene for the murine SCID defect. Science 267:1178-1183

Koyanagi Y, Tanaka Y, Kira J, Ito M, Hioki K, Misawa N, Kawano Y, Yamasaki K, Tanaka R, Suzuki Y, Ueyama Y, Terada E, Tanaka T, Miyasaka M, Kobayashi T, Kumazawa Y, Yamamoto N (1997a) Primary human immunodeficiency virus type 1 viremia and central nervous system invasion in a novel hu-PBL-immunodeficient mouse strain. J Virol 71:2417-2424

Koyanagi Y, Tanaka Y, Tanaka R, Misawa N, Kawano Y, Tanaka T, Miyasaka M, Ito M, Ueyama Y, Yamamoto N (1997b) High levels of viremia in hu-PBL-NOD-scid with HIV-1 infection. Leukemia 11 Suppl 3:109-112

Lu W, LC Arraes, WT Ferreira, J-M Andrieu (2004) Therapeutic dendritic-cell vaccine for chronic HIV-1 infection. Nat Med 10:1359-1365

Lu W, X Wu, Y Lu, W Guo, JM Andrieu (2003) Therapeutic dendritic-cell vaccine for simian AIDS. Nat Med 9:27-32

McCune JM, Kaneshima H, Krowka J, Namikawa R, Outzen H, Peault B, Rabin L, Shih CC, Yee E, Lieberman M et al. (1988) The SCID-hu mouse: murine model for the analysis of human hematolymphoid differentiation and function. Science 241:1632-1639

McCune JM, Kaneshima H, Krowka J, Namikawa R, Outzen H, Peault B, Rabin L, Shih CC, Yee E, Lieberman M et al. (1991) The SCID-hu mouse: a small animal model for HIV infection and pathogenesis. Annu Rev Immunol 9:399-429

McCune JM, Namikawa R, Shih CC, Rabin L, Kaneshima H (1990) Suppression of HIV infection in AZT-treated SCID/hu mice. Science 247:564-566

Miller RD, Hogg J, Ozaki JH, Gell D, Jackson SP, Riblet R (1995) Gene for the catalytic subunit of mouse DNA-dependent protein kinase maps to the scid locus. Proc Natl Acad Sci USA 92:10792-10795

Miura Y, Misawa N, Kawano Y, Okada H, Inagaki Y, Yamamoto N, Ito M, Yagita H, Okumura K, Mizusawa H, Koyanagi Y (2003) Tumor necrosis factor-related apoptosis-inducing ligand induces neuronal death in a murine model of HIV central nervous system infection. Proc Natl Acad Sci USA 100:2777-2782

Miura Y, Misawa N, Maeda N, Inagaki Y, Tanaka Y, Ito M, Kayagaki N, Yamamoto N, Yagita H, Mizusawa H, Koyanagi Y (2001) Critical contribution of TNF-related apoptosis-inducing ligand (TRAIL) to apoptosis of human $CD4^+$ T cells in HIV-1-infected hu-PBL-NOD-SCID mice. J Exp Med 193:651-659

Mori N, Fujii M, Ikeda S, Yamada Y, Tomonaga M, Ballard DW, Yamamoto N (1999) Constitutive activation of NF-kappaB in primary adult T-cell leukemia cells. Blood 93:2360-2368

Mosier DE, Gulizia RJ, Baird SM, Wilson DB (1988) Transfer of a functional human immune system to mice with severe combined immunodeficiency. Nature 335:256-259

Mosier DE, Gulizia RJ, Baird SM, Wilson DB, Spector DH, Spector SA (1991) Human immunodeficiency virus infection of human-PBL-SCID mice. Science 251:791-794

Mosier DE, Gulizia RJ, MacIsaac PD, Torbett BE, Levy JA (1993) Rapid loss of CD4+ T cells in human-PBL-SCID mice by noncytopathic HIV isolates. Science 260:689-692

Nakata H, Maeda K, Miyakawa T, Shibayama S, Matsuo M, Takaoka Y, Ito M, Koyanagi Y, Mitsuya H (2005) Potent Anti-R5-human immunodeficiency virus type 1 effects of a CCR5 antagonist, AK602/ONO4128/GW873140, in a novel human peripheral blood mononuclear cell nonobese diabetic-SCID, interleukin 2 receptor γ-chain-knocked-out AIDS mouse model. J Virol 79: 2087-2096

Namikawa R, Kaneshima H, Lieberman M, Weissman IL, McCune JM (1988) Infection of the SCID-hu mouse by HIV-1. Science 242:1684-1686

Nimura F, Zhang LF, Okuma K, Tanaka R, Sunakawa H, Yamamoto N, Tanaka Y (2006) Cross-linking cell surface chemokine receptors leads to isolation, activation, and differentiation of monocytes into potent dendritic cells. Exp Biol Med 231:431-443

Nonoyama S, Smith FO, Ochs HD (1993) Specific antibody production to a recall or a neoantigen by SCID mice reconstituted with human peripheral blood lymphocytes. J Immunol. 151:3894-3901

Osame M, Usuku K, Izumo S, Ijichi N, Amitani H, Igata A, Matsumoto M, Tara M (1986) HTLV-I associated myelopathy, a new clinical entity. Lancet 1:1031-1032

Pastore C, Picchio GR, Galimi F, Fish R, Hartley O, Offord RE, Mosier DE (2003) Two mechanisms for human immunodeficiency virus type 1 inhibition by N-terminal modifications of RANTES. Antimicrob Agents Chemother 47:509-517

Peterson SR, Kurimasa A, Oshimura M, Dynan WS, Bradbury EM, Chen DJ (1995) Loss of the catalytic subunit of the DNA-dependent protein kinase in DNA double-strand-break-repair mutant mammalian cells. Proc Natl Acad Sci USA 92:3171-3174

Rabin L, Hincenbergs M, Moreno MB, Warren S, Linquist V, Datema R, Charpiot B, Seifert J, Kaneshima H, McCune J (1996) Use of standardized SCID/hu Thy/Liv mouse model for preclinical efficacy testing of anti-human immunodeficiency virus type 1 compounds. Antimicrob Agents Chemother 40:755-762

Ruxrungtham K, Boone E, Ford H Jr, Driscoll JS, Davey RT Jr, Lane HC (1996) Potent activity of 2'-beta-fluoro-2',3'-dideoxyadenosine against human immunodeficiency virus type 1 infection in hu-PBL-SCID mice. Antimicrob Agents Chemother 40:2369-2374

Sandhu JS, Gorczynski R, Shpitz B, Gallinger S, Nguyen HP, Hozumi N (1995) A human model of xenogeneic graft-versus-host disease in SCID mice engrafted with human peripheral blood lymphocytes. Transplantation 60:179-184

Sandhu JS, Shpitz B, Gallinger S, Hozumi N (1994) Human primary immune response in SCID mice engrafted with human peripheral blood lymphocytes. J Immunol 152:3806-3813

Santini S M, C Lapenta, M Logozzi, S Parlato, M Spada, T Di Pucchio, F Belardelli (2000) Type I interferon as a powerful adjuvant for monocyte-derived dendritic cell development and activity in vitro and in Hu-PBL-SCID mice. J Exp Med 191:1777-1788

Stanley SK, McCune JM, Kaneshima H, Justement JS, Sullivan M, Boone E, Baseler M, Adelsberger J, Bonyhadi M, Orenstein J et al. (1993) Human immunodeficiency virus infection of the human thymus and disruption of the thymic microenvironment in the SCID-hu mouse. J Exp Med 178:1151-1163

Strizki JM, Xu S, Wagner NE, Wojcik L, Liu J, Hou Y, Endres M, Palani A, Shapiro S, Clader JW, Greenlee WJ, Tagat JR, McCombie S, Cox K, Fawzi AB, Chou CC, Pugliese-Sivo C, Davies L, Moreno ME, Ho DD, Trkola A, Stoddart CA, Moore JP, Reyes GR, Baroudy BM (2001) SCH-C (SCH 351125), an orally bioavailable, small molecule antagonist of the chemokine receptor CCR5, is a potent inhibitor of HIV-1 infection in vitro and in vivo. Proc Natl Acad Sci USA 98:12718-12723

Tary-Lehmann M and Saxon A (1992) Human mature T cells that are anergic in vivo prevail in SCID mice reconstituted with human peripheral blood. J Exp Med 175:503-516

Tary-Lehmann M, Saxon A, Lehmann PV (1995) The human immune system in hu-PBL-SCID mice. Immunol Today 16:529-533

Taylor GP, Matsuoka M (2005) Natural history of adult T-cell leukemia/lymphoma and approaches to therapy. Oncogene 24:6047-6057

Traggiai E, Chicha L, Mazzucchelli L, Bronz L, Piffaretti JC, Lanzavecchia A, Manz MG (2004) Development of a human adaptive immune system in cord blood cell-transplanted mice. Science 304:104-107

Uchiyama T, Hori T, Tsudo M, Wano Y, Umadome H, Tamori S, Yodoi J, Maeda M, Sawami H, Uchino H (1985) Interleukin-2 receptor (Tac antigen) expressed on adult T cell leukemia cells. J Clin Invest 76:446-453

Vandekerckhove BA, Namikawa R, Bacchetta R, Roncarolo MG (1992) Human hematopoietic cells and thymic epithelial cells induce tolerance via different mechanisms in the SCID-hu mouse thymus. J Exp Med 175:1033-1043

Watanabe S, Terashima K, Ohta S, Horibata S, Yajima M, Shiozawa Y, Dewan MZ, Yu Z, Ito M, Morio T, Shimizu N, Honda M, Yamamoto N (2007) Hematopoietic stem cell-engrafted NOD/SCID/IL2Rgamma null mice develop human lymphoid systems and induce long-lasting HIV-1 infection with specific humoral immune responses. Blood 109:212-218

Yoshida A, Tanaka R, Kodama A, Yamamoto N, Ansari AA, Tanaka Y (2005) Identification of HIV-1 epitopes that induce the synthesis of a R5 HIV-1 suppression factor by human CD4+ T cells isolated from HIV-1 immunized hu-PBL SCID mice. Clin Dev Immunol 12:235-242

Yoshida A, Tanaka R, Murakami M, Takahashi T, Koyanagi Y, Nakamura M, Ito M, Yamamoto N, Tanaka Y (2003) Induction of protective immune responses against R5 HIV-1 infection in the hu-PBL-SCID mice by intra-splenic immunization with HIV-1-pulsed dendritic cells: possible involvement of a novel factor of human $CD4^+$ T cell origin. J Virol 77:8719-8728

Zhang L, Kovalev GI, Su L (2007) HIV-1 infection and pathogenesis in a novel humanized mouse model. Blood 109:2978-2981

Microbiol Immunol 2008; **52**: 78–88
doi:10.1111/j.1348-0421.2008.00012.x

Human immunodeficiency virus type-1 vulnerates nascent neuronal cells

Hiroko Kitayama, Yoshiharu Miura, Yoshinori Ando and Yoshio Koyanagi

Laboratory of Viral Pathogenesis, Institute for Virus Research, Kyoto University, Kyoto 606-8507, Japan

Correspondence
Yoshio Koyanagi, Laboratory of Viral Pathogenesis, Institute for Virus Research, Kyoto University, 53 Shogoin-kawara-cho, Sakyo-ku, Kyoto 606-8507, Japan.
Tel: +81-75-751-4811; fax: +81-75-751-4812; email: ykoyanag@virus.kyoto-u.ac.jp

Received: 28 August 2007; accepted: 22 November 2007

List of Abbreviations: AIDS, acquired immunodeficiency syndrome; ART, antiretrovirus therapy; CNS, central nervous system; DG, dentate gyrus; EGFP, enhanced green fluorescent protein; FITC, fluorescein-isothiocyanate; GCL, granule cell layer; GFAP, glial fibrillary acidic protein; HIV-1, human immunodeficiency virus-1; NFP, neurofilament protein; NMDA, *N*-methyl-$_D$-aspartate; mAb, monoclonal antibody; MDM, monocyte-derived macrophages; MF, mossy fiber; MLV, murine leukemia virus; MOI, multiplicity of infection; NeuN, neuronal nuclei; O4, oligodendrocyte O4; OHC, organotypic hippocampal slice culture; PBMC, peripheral blood mononuclear cells; PCL, pyramidal cell layer; PFA, paraformaldehyde; RT, room temperature; tat, transcriptional transactivator; TUNEL, terminal deoxynucleotidyl transferase (TdT)-mediated biotinylated UTP nick end labeling; TNF-α, tumor-necrosis factor α.

Key words
dentate gyrus, HIV-1, neuron, organotypic hippocampal slice cultures.

ABSTRACT

Macrophages or microglial cells are the major target cells for HIV-1 infection in the brain. The infected cells release neurotoxic factors that may cause severe neuronal cell damage, especially in the basal ganglia and hippocampus. In this study, we used rat OHC to examine the region-specific neuronal cell damage caused by HIV-1-infected macrophages. When OHC was cocultured with HIV-1-infected MDM, we found that neuronal cells at the GCL of the DG were preferentially killed via apoptosis, and that projection of MF from GCL to PCL of the CA3 region was severely disturbed. We marked precursor cells around the DG region by using an EGFP-expressing retrovirus vector and found that these cells lost the ability to differentiate into neurons when exposed to HIV-1-infected MDM. In the DG, new neurons are normally incorporated into GCL or PCL, while in the presence of HIV-1-infected MDM, mature neurons failed to be incorporated into those layers. These data indicate that the neurotoxic factor(s) released from HIV-1-infected macrophages impede(s) neuronal cell repair in brain tissue. This suggests that DG is the region of the hippocampus most vulnerable to neuronal damage caused by HIV-1 infection, and that its selective vulnerability is most likely due to the highly active neurogenesis that takes place in this region.

HIV infection is well known to be a cause for development of dementia. Most HIV-associated dementia is subcortical dementia due to predominant involvement of the basal ganglia, cerebral cortex, and hippocampus (1–3). Introduction of ART has improved the immunological condition of patients and reduced the incidence of HIV severe dementia in AIDS patients (1, 4, 5). However, due to improved survival rates among ART-treated patients and healthy HIV-infected individuals, prevalence rates of HIV-1 associated neurological disease continue to rise (1). These patients display milder neurological disease than the severe neurological disease seen in non-treated patients

© 2008 The Societies and Blackwell Publishing Asia Pty Ltd

(1, 2). Histopathological examination of autopsy samples from HIV-1 infected brains reveals the presence of multinucleated giant cells and loss of synapses and neurons (6).

Although the mechanisms involved in loss of synapses and neurons in these patients are not completely understood, some data support the contention that HIV-1 infected macrophages or microglial cells release neurotoxic factors such as viral products, excitotoxins, and/or cytokines and chemokines that damage neurons through multiple pathways (1, 7). These factors may also work to activate astrocytes which then produce chemokines and cytokines that affect neuronal function (8, 9). Such neurotoxic factors are likely to affect a diverse range of neurons in the most vulnerable areas of the CNS, including the hippocampus, frontal cortex and white matter (1). In HIV-infected individuals, viral and host factors released from HIV-1-infected macrophages might affect hippocampal mediated learning and memory formation (1, 10). It has been reported that macrophage-induced inflammation affected hippocampal plasticity in a murine model of HIV-1 encephalitis (11). However, there has been no longitudinal study on the pathogenesis of HIV-1 encephalopathy and therefore no information has been collected by *in vitro* assay regarding the mechanism of causation of milder HIV-1 associated neurological disease.

As an *in vitro* model of HIV-1 encephalopathy that mimics its pathogenesis *in vivo*, OHC were employed in the present study. OHC would provide an alternative model to examine neuronal cell function in the hippocampus (12). As cellular composition, architecture and connections within the hippocampus are well preserved in OHC, the microenvironment in which the cells are immersed is similar to that in living animals (13–15). Although a few exceptions have been found, probably as a result of afferent deprivation of neuronal signals (16, 17), neurons in slice culture maintain their physiological arrangement and the capability to transmit signals (12). In addition, neurogenesis has been reported to occur in hippocampal slice cultures (18, 19). Therefore, slice cultures have been widely used to study morphology and plasticity of the hippocampus. Since HIV does not infect cells with a neuronal lineage, it was considered appropriate to use small animal-derived OHC in combination with HIV-1-infected human macrophages to study pathological changes in the brain of HIV-1-infected individuals.

In the present study, we established an *in vitro* model of HIV-1 encephalopathy using rat OHC exposed to HIV-1-infected MDM. This model reproduced pathological alterations such as neuronal apoptosis, loss of synapses and activation of astrocytes or microglial cells. More importantly, granule cells in the DG, where active neurogenesis occurs, were found to be predominantly damaged at an early stage, and neuronal cell differentiation was found to be disturbed by viral and/or host factors released from HIV-1-infected MDM. This culture system will be useful for understanding the pathology of HIV-1 encephalopathy in the hippocampus.

MATERIALS AND METHODS

OHC and cocultivation with HIV-1-infected macrophages

OHC were prepared from postnatal day seven Wister Hannover GALAS rats (CLEA, Osaka, Japan) as previously described (18). The experiments were carried out in accordance with the guidelines of Kyoto University for animal experimentation. After decapitation, the brain was removed and transversely sliced at the hippocampus into a 350 μm thickness on a McIlwain tissue chopper (Mickle Laboratory Engineering, Guildford, UK). The slices were cultured on porous translucent membrane (Millicell-CM, Millipore, Bedford, MA, USA) at 34°C and the culture medium was changed three times a week. The culture medium consisted of 50% OPTI-MEM (Invitrogen, Carlsbad, CA, USA), 25% heat inactivated horse serum (Invitrogen) and 25% Hank's balanced salt solution (Invitrogen) supplemented with $_{D}$-glucose (5 g/L, Wako, Osaka, Japan), penicillin and streptomycin (100 units/ml, 100 μg/ml, respectively, Invitrogen). Two weeks after initiation of culture, slices were cocultured with HIV-1_{JRFL} (20)-infected (MOI 1.0) or uninfected MDM isolated from PBMC of HIV-1 seronegative healthy donors, across the porous membrane in culture medium for another two weeks. The concentration of p24 antigen was measured by ELISA (RETROtek, ZeptoMetrix, Buffalo, NY, USA).

Retrovirus vector transduction

An MLV-based vector, SRα-EGFP (21), was derived from SRαL*thy* (22) by replacing the murine thy 1.2 gene with EGFP. Vector was generated as described before (21). The titer of vector was 1.7×10^7 infectious units per milliliter. Slices were inoculated with SRα-EGFP by microinjection (FemtJet and Inject Man NI2, Eppendorf, Hamburg, Germany) in the suprapyramidal region of the GCL at the DG (18). Then, slices were cultured without, or with uninfected or HIV-1-infected MDM, as described above.

Staining dead cells in OHC

After removal of culture medium, slices were incubated at 34°C with culture medium containing SYTOX Green dye (Invitrogen) for 30 min and then samples were examined using a fluorescent microscope (Nikon TS100, Nikon, Tokyo, Japan) using a GFP filter with 5× objective.

© 2008 The Societies and Blackwell Publishing Asia Pty Ltd

Antibodies

MAb against NeuN, nestin and O4 were purchased from Chemicon (Temecula, CA, USA). MAb against NFP and rat CD68 (clone ED1) were purchased from DakoCytomation (Carpinteria, CA, USA), and Serotec (Oxford, UK), respectively. A rabbit polyclonal antibody against GFAP was purchased from DakoCytomation. A rat mAb against EGFP was purchased from Nakarai (Kyoto, Japan). A biotin-conjugated goat anti-mouse IgM was purchased from Chemicon. Alexa Fluor 488-, 594-conjugated goat anti-mouse/rabbit IgG and Alexa Fluor 594-conjugated streptavidin were obtained from Invitrogen. An FITC-conjugated goat anti-rat IgG was obtained from Jackson Immuno Research Laboratories (West Grove, PA, USA).

Immunohistochemistry

Slices were fixed by immersion in 4% PFA for one hour at 4°C, and then incubated with blocking buffer containing 5% normal goat serum Vector Laboratories (Burlingame, CA, USA) and 0.3% Triton X-100 at 4°C overnight, followed by incubation with primary antibodies against the following molecules; NeuN, EGFP, NFP, rat CD68, O4, or GFAP at 4°C overnight in blocking solution. Sample stained with antibody against O4 was further incubated with biotin-conjugated anti-mouse IgM antibody at 4°C overnight. These samples were subsequently incubated at RT for another six hours with fluorescent dye conjugated secondary antibodies; Alexa Fluor 594-conjugated anti-mouse/rabbit IgG with or without FITC-conjugated anti-rat IgG or Alexa Fluor 594-conjugated streptavidin. Nuclei were stained using Hoechst33342 (Invitrogen). Each sample was examined under a fluorescent microscope (Leica CTR6500, Leica Microsystems, Heidelberg, Germany) using a Texas Red filter with 5× and 10× objectives, and a confocal laser microscope (TCS SP2 AOBS, Leica Microsystems) using 405, 488 or 543 nm excitations with 10×, 20× and 40× objectives. The quantification of fluorescent intensity was done following the protocol supplied by the manufacturer (LCS Lite software, Leica Microsystems).

TUNEL staining

Slices were fixed by immersion in 4% PFA for one hour at 4°C, treated with 20 mg/ml proteinase K in 50 mM Tris-HCl buffer at 37°C for 15 min, and then fixed again with 4% PFA for 30 min at 4°C. Following permeabilization with 0.3% Triton X-100 for one hour at RT, the samples were incubated with TdT solution (TdT buffer, 25 mM $CoCl_2$, TdT [Terminal Transferase recombinant, Roche Applied Science, Indianapolis, IN, USA], biotin-16-2′-deoxy-uridine-5′-triphosphate [Roche Applied Science]) at 37°C for four hours. After washing, samples were stained with anti-NeuN antibody as described above and subsequently incubated with fluorescent dye conjugated secondary antibodies: Alexa Fluor 488-conjugated anti-mouse IgG (NeuN) and streptavidin Alexa Fluor 594-conjugated (TUNEL). Nuclei were stained using Hoechst33342 at RT for six hours. Samples were examined under a confocal laser microscope using 405, 488 and 543 nm excitations with 20× and 40× objectives as described above.

RESULTS

Microscope analysis of OHC exposed with HIV-MDM

Since OHC is known to preserve morphological features of the CNS for at least one month, we used it to explore tissue damage caused by HIV-1 protein or humoral host factor produced by HIV-1-infected macrophages in the hippocampus. Typical cellular arrangement of granule cells was reconstituted in slices on a porous membrane 14 days after initiation of culture and slices were then exposed to HIV-1_{JRFL}-infected or uninfected MDM across the porous membrane for another 14 days. The laminated structure and morphological organization of slices cocultured with or without uninfected MDM was maintained during the 14 days (data not shown), while the slice exposed to HIV-1-infected MDM (HIV-MDM) was found to gradually become thinner (Fig. 1A). Although cell morphology of MDM was not changed by HIV-1 infection, high concentrations of HIV-1 even greater than 200 ng p24 antigen per milliliter were found in culture supernatant (Fig. 1A and B). In addition, moderate thinning down of slices was induced by exposure to culture supernatant of lower concentrations of p24 antigen (below 20 ng per milliliter) from HIV-1-infected MDM (data not shown). These results suggest that HIV-1-infected MDM produce factor(s) that impair the maintenance of neuronal tissue architecture.

HIV-1-induced region-specific damage of neuronal cells in the hippocampus

To examine which region was affected by HIV-1-infected MDM, OHC was cultured in the presence of a non-permeable staining reagent, SYTOX, and cell damage was examined. Two days after exposure to HIV-1-infected MDM, severe cell damage in the neuronal cell layer was found (Fig. 2A), suggesting that neurons in these regions were predominantly harmed at an early stage after exposure to HIV-1-infected MDM. Fourteen days after exposure, we found severe loss of neurons especially at the GCL of the DG as revealed by staining with antibody

© 2008 The Societies and Blackwell Publishing Asia Pty Ltd

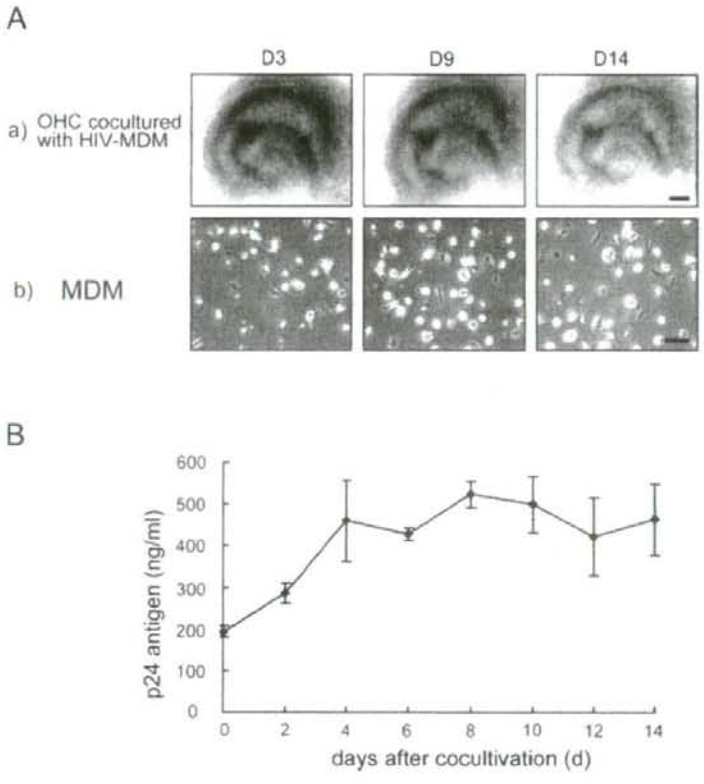

Fig. 1. Longitudinal alteration of OHC exposed to HIV-1-infected MDM. (A) OHC was cultured in the presence of HIV-1-infected MDM for two weeks. Microscopic examination was performed at days (D) 3, 9 and 14 after cocultivation. The slices gradually became thinner and cells were shed from them (a), though morphology of MDM was not affected by HIV-1 infection (b). Scale bar: 500 μm (a), 100 μm (b). (B) Large amount of HIV-1 was produced by HIV-1-infected MDM during cocultivation. X-axis is days after cocultivation and Y-axis is p24 concentration in supernatant of culture medium measured by ELISA.

against NeuN (Fig. 2B). Loss of GCL neurons was also found by staining with antibody against Calbindin D28K, one of the calcium binding proteins expressed specifically in GCL neurons (data not shown). Three-dimensional analysis revealed that the number of NeuN positive neurons clearly decreased and thickness of the sample became thinner in slices exposed to HIV-MDM compared to those without cocultivation (Fig. 2C). This change could not be found when OHC was exposed to HIV-1-infected HeLa-derived cells (data not shown), indicating that loss of neurons was specific to HIV-1-infected MDM and that exposure to HIV-1-infected MDM was more effective in reproducing the pathological alteration of HIV-1 encephalopathy. These results suggest that humoral factor(s) produced from HIV-1-infected MDM preferentially damage cells in the DG.

Neuronal apoptosis in the DG induced by HIV-1-infected MDM

To investigate the mechanism involved in the reduction in number of neurons especially at the DG region, we next carried out TUNEL staining to examine whether these cells were killed via apoptosis. There were many TUNEL positive cells in $NeuN^+$ neurons localized at the DG region in slices exposed to HIV-1-infected MDM (Fig. 2D and E). By contrast, in slices exposed to uninfected MDM, there were less TUNEL positive neurons in PCL and GCL. Furthermore, in slices exposed to uninfected MDM, there was no difference in the number of TUNEL positive cells between PCL (CA1 and CA3) and GCL (DG) (Fig. 2E). These data indicate that granule cells in the DG area are highly susceptible to apoptosis which is probably induced by neurotoxic humoral factor released from HIV-1-infected MDM.

Synaptic loss of GCL neurons induced by HIV-1-infected MDM

We assumed that other mechanisms besides neuronal apoptosis induced neuronal damage at the DG in OHC. To confirm this assumption, we used NFP as a marker to visualize neuronal filaments such as axons and dendrites. In slices exposed to HIV-1-infected MDM, expression of NFP was severely disturbed at the DG region (Fig. 2F and G).

© 2008 The Societies and Blackwell Publishing Asia Pty Ltd

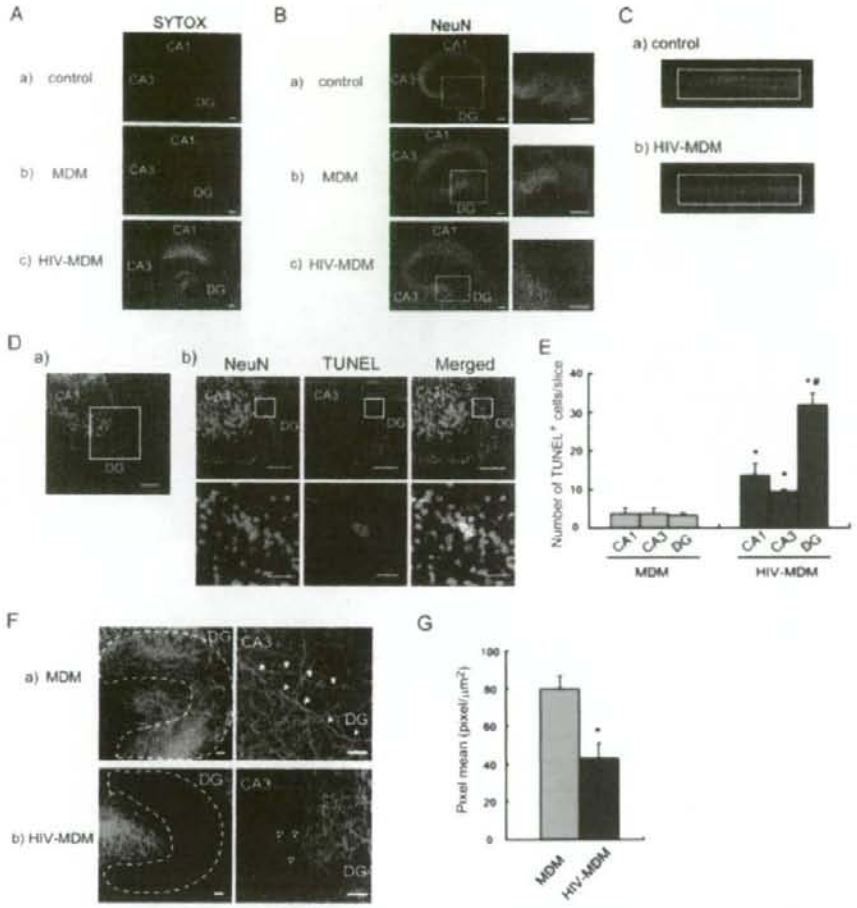

Fig. 2. Neurotoxic effect in OHC exposed to HIV-1-infected MDM. (A) Neurons in the CA1 and DG were harmed at early stage after the initiation of the exposure to HIV-1-infected MDM. Slices were cultured without (a; control) or with uninfected (b; MDM) or HIV-1-infected MDM (c; HIV-MDM) for two days and stained with SYTOX. CA1: CA1 region, CA3: CA3 region, DG: dentate gyrus. Scale bars: 100 μm. (B) Severe loss of neurons at the GCL of the DG was found in OHC exposed to HIV-1-infected MDM. Slices were cultured without (a; control) or with uninfected (b; MDM) or HIV-1-infected MDM (c; HIV-MDM) for 14 days and stained with antibody against NeuN. Rectangular regions were enlarged. CA1: CA1 region, CA3: CA3 region, DG: dentate gyrus. Scale bars: 100 μm. (C) Thinning of slices and loss of neurons were found by three-dimensional analysis in OHC exposed to HIV-1-infected MDM. Slices were cultured without (a; control) or with HIV-1-infected MDM (b; HIV-MDM) for 14 days and stained with NeuN (neuron) and Hoechst33342 (nuclei). The x-z plane of slices was imaged using a fluorescent microscope. (D) Neuronal apoptosis was induced by HIV-1-infected MDM. Slices cultured with HIV-1-infected MDM were stained with TUNEL (red) and anti-NeuN antibody (green), and nuclei were stained with Hoechst33342 (blue). A low magnification image is shown in left panel (a), and a high magnification image is shown in right panel (b). Rectangular regions were enlarged. CA3: CA3 region, DG: dentate gyrus. Scale bars: 150 μm (a), 100 μm (b, upper panels), 25 μm (b, lower panels). (E) Neuronal apoptosis was induced especially at the GCL of the DG. The numbers of TUNEL positive neurons were counted at three areas (CA1, CA3 and DG) of the slices cultured with uninfected (MDM) or HIV-1-infected MDM (HIV-MDM). Y-axis indicates the number of TUNEL positive neurons in slice.*: $P < 0.01$ versus each area of MDM, #: $P < 0.01$ versus CA1 and CA3 in HIV-MDM. (F) Loss of synapses was induced in GCL neurons by HIV-1-infected MDM. Slices cultured with uninfected (a; MDM) or HIV-1-infected MDM (b; HIV-MDM) were stained using antibody against NFP and neuronal filaments were visualized. Low magnification images are shown in left panels, and high magnification images in right panels. The area enclosed by the dotted line indicates the DG area. Long axons were formed (filled arrowheads) in GCL neurons at DG and they projected to CA3 in slice cultured with uninfected MDM (a). Conversely, axons were severely damaged (open arrowheads) in GCL neurons of DG in slice cultured with HIV-1-infected MDM (b). Scale bars: 50 μm. (G) Pixel mean of the signal of NFP-stained samples was significantly decreased in the slices cultured with HIV-1-infected MDM (HIV-MDM). *: $P < 0.01$ versus uninfected MDM (MDM).

© 2008 The Societies and Blackwell Publishing Asia Pty Ltd

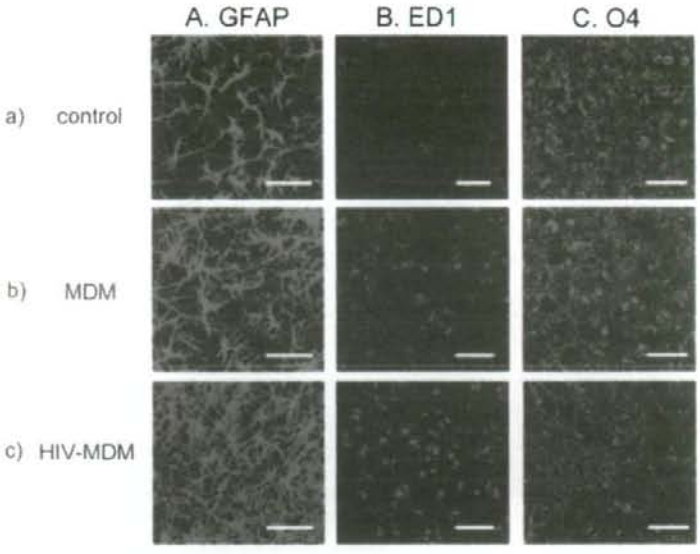

Fig. 3. Abnormality in astrocytes, microglial cells, and oligodendrocytes. Slices were cultured without (a; control) or with uninfected (b; MDM) or HIV-1-infected MDM (c; HIV-MDM) for 14 days and stained using antibodies against GFAP (A), ED1 (B) and oligodendrocyte O4 (C). The number of astrocytes increased in the presence of HIV-1-infected MDM (A), and the number of microglial cells increased and morphological changes were found when exposed to HIV-1-infected MDM (B). Conversely, oligodendrocytes were damaged by HIV-1-infected MDM (C). Scale bars: 50 μm.

Furthermore, the MF, collateral sprouting of dentate granule cell axons which form powerful excitatory synapses onto the proximal dendrites of CA3 pyramidal cells (23), were severely damaged in slices exposed to HIV-1-infected MDM (Fig. 2F, open arrowheads) as compared to uninfected MDM (Fig. 2F, filled arrowheads), indicating that HIV-1-infected MDM induce malformation of neuronal filaments and abnormality of synaptic projection onto neurons.

Activation of astrocytes or microglial cells and depletion of oligodendrocytes by HIV-1-infected MDM

We reproduced neuronal tissue damage through neuronal apoptosis and axonal malformations by exposure to HIV-1-infected MDM in the region of the DG. Other types of cells in OHC, which also includes astrocytes, microglial cells and oligodendrocytes, were also examined. It has been reported that astrocytes and microglial cells are extraordinarily activated in the brains of HIV-1 encephalopathy patients (2). From examination of GFAP (astrocyte marker), rat CD68 (microglial cell marker) and O4 (oligodendrocyte marker) expressions using immunofluorescence techniques, we found enlarged astrocytes and microglial cells in the slices exposed to HIV-1-infected MDM, indicating that astrocytes and microglial cells were activated (Fig. 3A and B). In addition, in the slices exposed to uninfected MDM, astrocytes and microglial cells were slightly enlarged, suggesting that both uninfected and HIV-1-infected MDM produce the factor(s) that induce activation of astrocytes and microglial cells (Fig. 3A and B). By contrast, the number of oligodendrocytes was clearly decreased in slices exposed to HIV-1-infected MDM, indicating that oligodendrocytes were preferentially damaged as seen in neurons by HIV-1-infected MDM (Fig. 3C). These results indicate that OHC cocultured with HIV-1-infected MDM is an adequate model for investigation of the molecular mechanism of HIV-1 encephalopathy.

Disablement of neuronal cell differentiation by HIV-1-infected MDM

It has become known that active neurogenesis occurs in the DG region of the hippocampus throughout the lifespan and that it is crucial for formation of neuronal plasticity (24). Many neuronal and glial progenitor cells or stem cells reside in the region and intrinsic and spontaneous neurogenesis are reported to take place at the DG in OHC (18, 19). In a healthy hippocampus, damaged neurons are continuously replaced by new cells generated at the DG region. However, in HIV-1-infected MDM-exposed slices, the damaged cells as shown in Figure 2 might accumulate as a result of weakened replacement. There could be two explanations for this observation. One is that the total number of precursors including progenitor cells and stem cells in DG decrease as a result of exposure to HIV-1-infected MDM. Another is that HIV-1-infected MDM interferes with the ability of precursor cells to differentiate and migrate.

© 2008 The Societies and Blackwell Publishing Asia Pty Ltd

To examine the first possibility, progenitor cells in the slices were stained with antibody against nestin, which is expressed predominantly in precursors including stem or progenitor cells of the CNS. We found similar numbers of nestin$^+$ precursor cells in slices exposed to either uninfected or HIV-1-infected MDM (Fig. 4A-a, b), indicating that factor(s) produced from HIV-1-infected MDM did not preferentially kill the precursors. To examine the second possibility, we labeled endogenous precursors in the slices using EGFP-expressing MLV vector (SRα-EGFP), which was microinjected into the suprapyramidal region of the GCL. Since MLV only infects dividing cells, and its DNA is incorporated into the host DNA, newly divided cells would specifically express EGFP. After inoculation with SRα-EGFP, slices were exposed to HIV-1-infected or uninfected MDM or not exposed to MDM at all. The total numbers of EGFP-expressing cells in all slices were similar irrespective of exposure of HIV-1-MDM or not for 2 weeks post inoculation (data not shown). To examine the ability of neuronal cell to differentiate, slices were fixed and stained with anti-NeuN antibody (neuron marker) and anti-EGFP antibody. In the slices cultured with uninfected MDM, some EGFP$^+$ cells also expressed NeuN and were incorporated into the GCL or PCL (Fig. 4B-a), and those cells had axon-like processes (Fig. 4B-a, filled arrowheads). Measurement of the numbers of EGFP$^+$ NeuN$^+$ neurons incorporated into the GCL or PCL revealed that half of EGFP$^+$ cells were neurons and those cells were incorporated into neuronal cell circuit in slices cultured with or without uninfected MDM (Fig. 4C). By contrast, in slice exposed to HIV-1-infected MDM, the majority of EGFP$^+$ cells were not incorporated into the GCL or PCL (Fig. 4B-b and C). Furthermore, EGFP$^+$ cells which were not incorporated into those layers did not express NeuN (Fig. 4B-c and C), indicating that EGFP$^+$ cells could not differentiate into mature neurons and that they might have differentiated into other cell types. These results indicate that maintenance of neuronal cell circuits is disturbed by exposure to HIV-1-infected MDM through inhibition of neuronal cell differentiation, but not by elimination of their progenitors in the DG.

DISCUSSION

In this study, we established a cocultivation system employing HIV-1-infected MDM and rat OHC that reproduces pathologic changes of HIV-1 encephalopathy. Neuronal dysfunctions including neuronal apoptosis and synaptic loss were produced especially in the GCL of the DG region in the hippocampus. Furthermore, in the DG, the differentiation of precursor cells into neurons was inhibited by exposure to HIV-1-infected MDM. These results highlight that the DG is profoundly susceptible to HIV-1 caused neuronal damage, and that HIV causes hippocampal dysfunction through damaging preexisting mature neurons and inhibiting the production of new neurons.

It has been reported that culture systems of a combination of OHC and HIV-1-encoded proteins, such as HIV-1-envelope glycoprotein 120 (gp120) or Tat, are useful for the study of HIV-1-induced neuronal damage (25–27), and that neuronal toxicity is induced by those viral proteins. Those culture systems are satisfactory for understanding the mechanisms by which a single protein affects maintenance of neuronal tissue. However, in the brain of HIV-1-infected patients, there are several viral proteins as well as host factors released from HIV-1-infected macrophages or microglial cells. Our coculture system using OHC and HIV-1-infected macrophages may reflect the brain damage which is concomitantly induced by several viral proteins and/or many host factors released from HIV-1-infected MDM. The combination of OHC and HIV-1-infected MDM may be more effective for identifying the mechanisms of HIV-1 encephalopathy. Moreover, in our coculture system, OHC might be exposed to high concentrations of viral and host factors and neuronal damage or degeneration thus induced, though neuronal damage was also found from exposure to a lower concentration of p24 antigen of culture supernatant. In the HIV-1-infected brain, HIV-1-infected macrophages penetrate across the blood-brain-barrier (2). More severe damage is induced around the area invaded by infected macrophages compared to uninvaded areas, as shown in simian immunodeficiency virus-infected brain samples (28). Our coculture system might reflect alterations which are closely related to those in areas invaded by HIV-1-infected macrophages.

Infected macrophages and microglial cells are known to be major HIV producers. They are also known to release viral proteins that can be deleterious to the CNS. HIV-1gp120, Tat and viral protein R have been shown to be toxic to neurons (29–33). HIV-1 gp120 interacts with cellular receptors and alters the signaling of the glutamate pathway. The signal induces cytokine production that can damage large number of neurons and affect the activation state of microglial cells and astrocytes (1). Nanomolar concentrations of gp120 have been reported to interact with the glycine binding site of the NMDA receptor (34). One possible molecular mechanism for gp120-induced neurotoxicity is that gp120 might induce glutamate-mediated excitotoxicity and initiate caspase cascades (35). Another viral protein Tat directly enters granule cells in the hippocampus and causes neurotoxicity (30). The neurotoxic effects of Tat seem to be mediated by interactions with a polyamine-sensitive site of the NMDA receptor in OHC (27). Infected cells also produce other neurotoxic

© 2008 The Societies and Blackwell Publishing Asia Pty Ltd

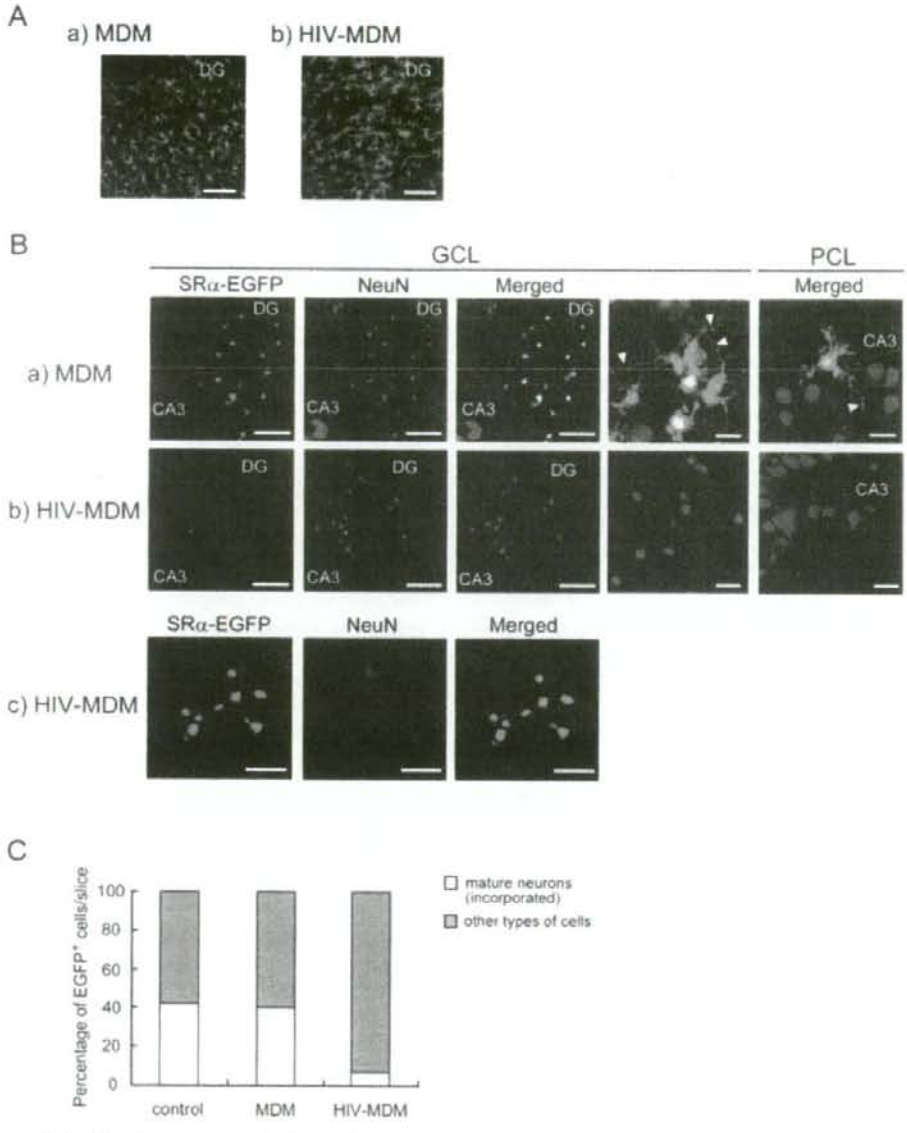

Fig. 4. Abnormality in differentiation ability of precursor cells. (A) The number of precursors was not affected by HIV-1-infected MDM. Slices were cultured with uninfected MDM (a; MDM) or HIV-1-infected MDM (b; HIV-MDM) for 14 days and stained using antibody against nestin to visualize endogenous precursors. CA3: CA3 region, DG: dentate gyrus. Scale bars: 50 μm. (B) Maturation of precursor cells into neurons was strongly inhibited in the presence of HIV-1-infected MDM. Precursor cells were labeled using an EGFP-expressing MLV vector and slices were cultured with uninfected (a; MDM) or HIV-1-infected MDM (b and c; HIV-MDM). Slices were stained using antibody against EGFP (green) and NeuN (red). EGFP$^+$ cells also expressed NeuN and had axon-like processes (filled arrowheads) in slices exposed to uninfected MDM (a, GCL and PCL). Conversely, EGFP$^+$ cells did not express NeuN and the number of EGFP$^+$ cells, which were incorporated into GCL or PCL clearly decreased in slices exposed to HIV-1-infected MDM (b, c). granule cell layer (GCL), pyramidal cell layer (PCL), CA3: CA3 region, dentate gyrus (DG). Scale bars, 100 μm, 20 μm (GCL right panels and PCL panels). (C) HIV-1-infected MDM induced abnormality of neuronal cell differentiation. Slices were cultured and stained using antibodies against EGFP and NeuN as described in B. The number of total EGFP$^+$ cells and EGFP$^+$/NeuN$^+$ cells which were incorporated into GCL or PCL were counted and classified into mature neurons (incorporated to neuronal circuit) or cells other than mature neurons. Y-axis indicates percentage of EGFP$^+$ cells in slice.

© 2008 The Societies and Blackwell Publishing Asia Pty Ltd

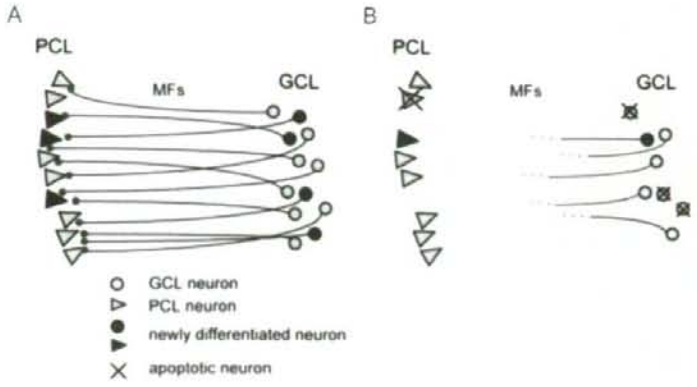

Fig. 5. Proposed model of HIV-1-infected macrophage-induced neuronal damage at the DG region. (A) In a normal OHC, MFs of GCL neurons (open dots) project to PCL neurons (open triangles) at CA3. New neurons differentiated from precursors were incorporated and configured in neuronal circuit (filled dots and triangles). (B) Conversely, in OHC exposed to HIV-1-infected macrophages, neurons underwent apoptosis (crossed dots and triangles) and MFs of GCL neurons (open dots) could not project to PCL neurons (open triangles) at CA3. However, precursors, which have the ability to replace damaged neurons, lose their ability to differentiate into neurons and can not be incorporated into GCL or PCL. Therefore, the damaged neurons and lost neuronal connections may accumulate in the DG region of hippocampus.

factors, such as cytokines including TNF-α, quinolinic and arachidonic acid, platelet-activating factor and nitric oxide (2, 36–38). These factors promote further activation of macrophages and/or microglial cells, as well as proliferation and activation of astrocytes (2). In addition, activated astrocytes release intracellular Ca^{2+} and glutamate while reducing the uptake of glutamate. This raises the extracellular concentration of glutamate and other neurotoxins that can induce excitotoxic death of neurons (39, 40). As a result, neurodegeneration may be accelerated in the HIV-1 infected brain (2, 6). We found that HIV-1-infected MDM induces damage in neuronal cells at an early stage of exposure (Fig. 2). At a later point, neuronal apoptosis, synaptic loss, impairment of oligodendrocytes and activation of astrocytes and microglial cells are induced by HIV-1-infected MDM (Figs 2, 3). These phenomena are probably caused by several virion-free viral proteins, such as gp120 and Tat, which are known to interact with several receptors and induce neurotoxic signaling, causing release of many host factors, such as TNF-α, from HIV-1-infected MDM. As a result, observed changes in OHC after exposure to HIV-1-infected MDM are very similar to some of the pathological alterations detected in the brain with HIV-1 encephalopathy.

In Borna disease and Alzheimer's disease, the greatest tissue damage is reported to be localized in the DG of hippocampus (41, 42). Thus, the DG region appears to be predisposed to neuronal damage, including that induced by HIV-1 infection. The DG is one of the unique regions where new neurons are continuously generated throughout life (24, 43). Neural stem cells derived from the adult hippocampus differentiate into neurons and form synaptic networks (24). These morphological and physiological features strongly suggest that new neurons are incorporated into the local circuitry of the hippocampus and that they are involved in hippocampus-dependent memory formation and brain repair (24, 44, 45). We found that differentiation of precursors (general progenitor cells and stem cells) into neurons was significantly impaired at the DG region by exposure to HIV-1-infected MDM, and that new neurons were scarcely incorporated into neuronal circuits (Fig. 4). As a result, the number of neurons might be reduced because new neurons are not being supplied from the DG region. Although the number of new neurons was significantly reduced, their precursors were not affected by HIV-1-infected MDM, suggesting that precursors may have been directed toward the differentiation pathway that leads to the production of astrocytes rather than neurons. Then, it can be assumed that apoptosis or synaptic loss caused by exposure to HIV-1-infected MDM results in progressive neuronal degradation because the injured neurons are not replaced (Fig. 5). Selective inhibition of neuronal differentiation might be mediated by several viral proteins or many neurotoxic host factors. HIV-1 gp120 interacts with NMDA receptors, and induces disruption of glutamate and glycolytic pathway signaling and calcium homeostasis (1). NMDA receptors are frequently expressed on immature granule neurons, and signals via NMDA receptors regulate neurogenesis and neuronal migration in the hippocampus both *in vitro* and *in vivo* (46–48). When HIV-1 gp120 interacts with NMDA receptors in immature neuronal precursor cells, neurogenesis is impaired. It has been considered that TNF-α released from infected macrophages plays a role in the process of neuronal damage. TNF-α inhibits phosphorylation of three signaling molecules, serine/threonine protein kinase, extracellular signal-related kinase and glycogen synthase kinase 3β, which are

© 2008 The Societies and Blackwell Publishing Asia Pty Ltd